ARTICLE

Photoemission Studies of High-T_c Superconductors: The Superconducting Gap

Z.-X. Shen, W. E. Spicer, D. M. King, D. S. Dessau, B. O. Wells

Over the last several years there have been great improvements in the energy resolution and detection efficiency of angle-resolved photoemission spectroscopy. These improvements have made it possible to discover a number of fascinating features in the electronic structure of the high transition temperature (T_c) superconductors: apparently bandlike Fermi surfaces, flat-band saddle points, and nested Fermi surface sections. Recent work suggests that these features, previously thought explainable only by one-electron band theory, may be better understood with a many-body approach. Furthermore, other properties of the high-T_c superconductors, which are difficult to understand with band theory, are well described using a many-body picture. Angle-resolved photoemission spectroscopy has also been used to investigate the nature of the superconducting pairing state, revealing an anisotropic gap consistent with a *d*-wave order parameter and fueling the current debate over *s*-wave versus *d*-wave superconductivity.

The excitement following the discovery of high-temperature superconductivity (*1*, *2*) was shared between those who saw an opportunity to finally take advantage of the unique properties of a superconductor at an economical price and those who wondered why metal oxides, normally good insulators, would superconduct at temperatures higher than thought possible for metals and alloys. The excitement has diminished for proponents of quick practical applications because progress has proceeded more slowly than the optimistic initial speculations. However, the excitement has endured within the solid-state physics community where fundamental issues are still being addressed, for example, the impact of the strong Coulomb interaction in these materials on the electronic structure and the microscopic origins for superconductivity.

One of the most difficult problems in physics, which has remained unsolved since the formulation of quantum mechanics, is understanding electron transport and the electronic structure in highly correlated systems where the electron-electron Coulomb interactions are very strong. Two distinct approaches have been used to address this problem (*3*–*6*). The first approach, known as band theory, uses delocalized wave functions to describe the electrons and a mean-field potential to approximate the electron-electron interactions. Sophisticated first principles calculations based on band theory have proven to be an extremely powerful tool for quantitative predictions and a qualitative understanding of the electronic structure in semiconductors and simple metals. However, band theory fails for certain classes of materials that contain partially occupied localized orbitals and may need to be supplanted with a theory that better accounts for many-body effects. The other approach accounts for the many-body effects in the localized orbitals by explicitly incorporating the strong Coulomb interactions among the electrons, usually with the use of highly idealized theoretical models. Typically, such an approach assumes that there is only one spatial state available per unit cell and includes an on-site Coulomb interaction between electrons with opposite spins to account for magnetic and correlation effects. For undoped materials, each site is singly occupied because the energy U required to place two carriers on a site is large. Doping adds additional carriers, creating doubly occupied sites, which may then hop to neighboring sites, provided they are not already doubly occupied. Unfortunately, this model is extremely difficult to work with and is no longer based on first principles. Interest in this challenging problem has been renewed because it appears to be the key to a microscopic understanding of high-T_c superconductivity.

All of the known high-T_c superconductors contain CuO_2 planes (Fig. 1A), where the superconducting carriers travel, separated by intermediate layers, which stabilize the lattice and act as charge reservoirs. An extremely simple band calculation based on the structure in Fig. 1A leads to the bands illustrated in Fig. 1B and predicts a simple diamond-shaped Fermi surface at half filling (Fig. 1C). The saddle-point at (π, 0) produces a van Hove singularity in the density of states (Fig. 1D). We know that this model is inadequate because the metallic behavior predicted at half-filling contradicts the experimental observation of a 2-eV insulating band gap. This failure is believed to result from the strong Coulomb interaction between conduction electrons, which is not accounted for correctly in the band calculation. The insulating nature of these systems can be explained qualitatively by a simple model named after Hubbard. In this

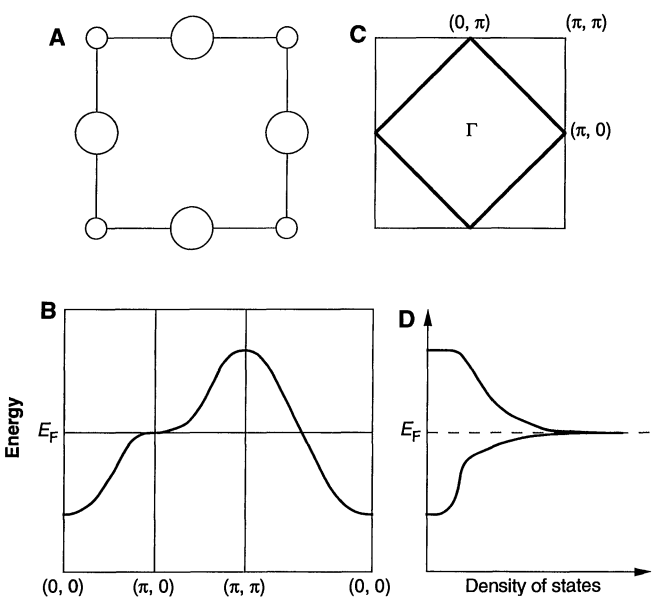

Fig. 1. (**A**) The crystal structure of the CuO_2 plane. The small circles represent the copper atoms, and the large circles represent the oxygen atoms. (**B**) Energy E versus wave vector **k** for the band with a saddle point at (π, 0). (**C**) The crystal's first Brillouin zone. The diamond-shaped thick lines show the Fermi surface at half-filling. (**D**) At half-filling, the Fermi level sits at the saddle point and creates a van Hove singularity in the density of states at the Fermi energy E_F.

Z.-X. Shen, Department of Applied Physics and Solid State Laboratory, Stanford University, Stanford, CA 94305, and Stanford Synchrotron Radiation Laboratory, Stanford, CA 94309–0210, USA. W. E. Spicer and D. M. King, Stanford Synchrotron Radiation Laboratory, Stanford, CA 94309–0210, and Solid State Laboratory, Stanford University, Stanford, CA 94305, USA. D. S. Dessau, Stanford Synchrotron Radiation Laboratory, Stanford, CA 94309–0210, USA. B. O. Wells, Physics Department, Massachusetts Institute of Technology, Cambridge, MA 02139, USA.

model, a strong Coulomb repulsion suppresses charge fluctuations that lead to double occupancy on localized sites. When the Coulomb interaction U exceeds the bandwidth W, the system becomes an insulator even though the band is only half-filled. These materials are called Mott insulators. When the cuprates are doped away from half-filling, they become superconductors; therefore, the high-T_c superconductors are often called doped Mott insulators.

While it is generally accepted that the electronic structure of high-T_c superconductors cannot be fully described with either a band (delocalized) or an idealized many-body (localized) picture, the issue under debate is whether one should approach it starting from the localized or delocalized limit. The theories that advocate the localized picture emphasize their connection to Mott insulators. Some of these theories further state that, because of the observation of many unconventional physical properties in these superconductors, we may be dealing with a new state of matter. On the other hand, the delocalized approach argues that, because of doping, the superconductors are qualitatively different from insulators and can be understood within the framework of band theory with small renormalizations. There are many excellent review articles describing the details and successes of both one-electron and many-body approaches (*7–9*).

The importance of the strong Coulomb interaction in these superconductors is directly related to the current debate over the superconducting pairing mechanism. It has been accepted for some time that high-T_c superconductivity is associated with the formation of Cooper pairs, as in conventional Bardeen-Cooper-Schrieffer (BCS) superconductors. The question under scrutiny is the nature of the microscopic pairing mechanism. For low-T_c superconductors, where the pairing is mediated by the isotropic electron-phonon interactions, the superconducting state is mostly isotropic, and the pair wave function has an orbital angular momentum of $l = 0$ (s wave). For high-T_c superconductors, strong Coulomb and related magnetic interactions are predicted to produce an anisotropic pairing state (*10–18*). Some theories further suggest that the pairing state is d wave ($l = 2$) (*10–12, 16–18*). Early experiments carried out on lower quality samples found an isotropic pairing state (*19*).

This article describes recent information we have acquired on the electronic structure and the pairing state from angle-resolved photoemission spectroscopy (ARPES) experiments, which were made possible by significant advances in instrumentation (*20–45*). In the superconductors, interesting features in the electronic structures have been discovered near the Fermi level: apparently bandlike Fermi surfaces, significantly less quasi-particle dispersion than predicted by band calculations, the presence of an extended saddle point near the Fermi level, and Fermi surfaces with strong nesting features. A critical analysis of experimental data in light of recent advances in many-body theory shows that effects previously thought to be explained by band theory alone (such as the large Fermi surface) may also be accounted for by an idealized many-body approach. In addition, there are many elements of the data that can be better described with the use of many-body approaches. Therefore, it appears that it will be necessary to go beyond one-electron theory to understand the electronic structure of the cuprates. Recent ARPES data from $Bi_2Sr_2CaCu_2O_8$ (Bi2212) in the superconducting state and other experimental data from higher quality $YBa_2Cu_3O_7$ (YBCO123) reveal a gap that is very anisotropic and is consistent with d-wave theory (*20*).

Photoemission Experiment and Normal-State Electronic Structure

In a photoemission experiment, incident photons excite electrons above the vacuum level so that they can be collected and energy analyzed. A typical valence-band photoemission spectrum from a single-band material consists of a peak and some background. The kinetic and binding energies of the electron are determined by the peak energy position. The crystal momentum is determined by the simple expressions $|\mathbf{k}| = (2mE_{kin}/\hbar^2)^{1/2}$ and $k_{\parallel} = |\mathbf{k}| \sin\theta$, where m is the mass of the electron, E_{kin} is its kinetic energy, $\hbar$ is the Planck constant, and θ is the angle of the emitted electron with respect to the surface normal. By taking spectra at many angles, a relation between E_{bin} and $\mathbf{k}$ can be obtained, where $E_{bin} = E_{photon} - E_{kin}$ is the binding energy of the electron. For two-dimensional materials, which the layered cuprates approximate, E_{bin} versus $k_{\parallel}$ is sufficient to determine the band structure throughout the Brillouin zone.

Photoemission studies of superconductors are experimentally demanding because both very high energy resolution and very good surface quality are required (*46*). Compounds like Bi2212, which have planes separated by weak van der Waals bonds, are extremely easy to cleave and expose a surface that is representative of the bulk, as verified by low-energy electron diffraction and scanning tunneling microscopy. A full ARPES spectrum of a cuprate consists of a main valence band 6 to 7 eV wide with strong intensity, a weak satellite at a binding energy of about 12 eV, and a small "foot" near the Fermi level. The overall spectrum can only be understood by considering both the O 2p and Cu 3d states (*47–50*). The satellite at 12 eV has no explanation in band theory and is believed to be a direct testimony of a large Coulomb interaction U, estimated to be 6 to 8 eV from photoemission spectra (*47–49*). We will consider only the foot because it is the band of lowest energy and is most relevant to the physical properties and electronic structure issues presented in Fig. 1. Because this foot is a mixture of Cu 3d and O 2p states, the Hubbard model should be regarded as the effective one-band model for the mixed states.

Early on, it was thought that a possible test of the applicability of one-electron theory and many-body theory was to measure the size and shape of the Fermi surface.

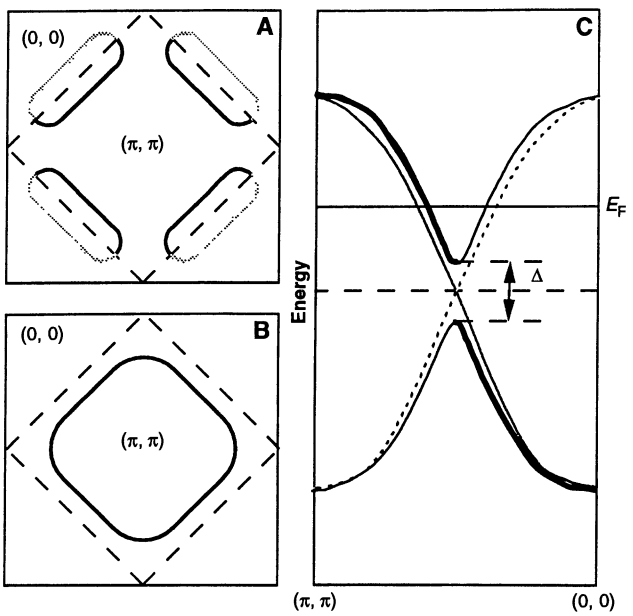

Fig. 2. (**A**) Naïve picture of the doped Fermi surface of a Mott insulator. The portion of the Fermi surface corresponding to the original band has stronger oscillator strength (thick lines). (**B**) The Fermi surface of a doped cuprate as expected from band theory. (**C**) SDW analogy of the insulating gap formation. The bands corresponding to the original band have higher oscillator strength (thick lines).

Several many-body theoretical calculations predicted that the Fermi surface would form small pockets centered at $(\pi/2, \pi/2)$ (Fig. 2A), in contrast to the large Fermi surface predicted by the one-electron approach (Fig. 2B).

Johnson *et al.* (*23*) first revealed the existence of a Fermi level using angle-integrated photoemission. The ARPES studies of the cuprates began with metallic and superconducting samples (*24*). The first high-resolution ARPES data, which made a significant impact on our understanding of the Fermi surface, was the work by Olson *et al.* on $Bi_2Sr_2CaCu_2O_{8+\delta}$(Bi2212) (*25*). After this pioneering study, many groups performed more detailed studies of the cuprate compounds and found qualitatively similar results (*26–34*). For simplicity, we present here the results of $Nd_{2-x}Ce_xCuO_{4+\delta}$ (NCCO), which is a paradigm compound that contains only one CuO_2 plane per unit cell and is electron doped (*n* type) (*30*, *33*). Figure 3 reproduces the angle-resolved photoemission data from NCCO by Anderson *et al.* (*30*) and King *et al.* (*33*). Moving from (0, 0) toward (π, π), we see a band dispersing toward the Fermi level that eventually crosses the Fermi level at $(0.44\pi, 0.44\pi)$. This Fermi level crossing point reveals the Fermi surface location along this direction. The experimental Fermi surface agrees with the calculated Fermi surface by Massidda *et al.* (*51*), which is based on one-electron band theory.

For other compounds, the experiments also reveal large Fermi surfaces, but the agreement between the data and band theory is not as good as in Fig. 3. The three compounds Bi2212, $Bi_2Sr_2CuO_6$ (Bi2201), and NCCO (*52*) appear to have large Fermi surfaces (Fig. 4) that can be considered as rounded versions of the diamond Fermi surfaces presented in Fig. 1C. Both Bi2212 and Bi2201 show long sections of the Fermi surfaces that are parallel to one other, which is usually called Fermi surface nesting. This might be responsible for some of the unconventional physical properties found in these superconductors (*53*). The role of Fermi surface nesting in high-T_c superconductors is further corroborated by the scaling of spin susceptibility as a function of the frequency divided by the temperature as observed in neutron-scattering experiments (*53*, *54*). On the other hand, NCCO does not exhibit any nesting features in its Fermi surface. This is consistent with the conventional normal-state properties found in this compound.

The simple observation of a Fermi surface has made a significant impact on the understanding of these materials (*7*, *9*). At face value, these experiments suggest that the high-T_c superconductors have large Fermi surfaces. This agreement between experiment and band theory predictions was hailed as a triumph for band theory (*9*). However, recent advances in many-body theories have shown that it is possible to reconcile the large Fermi surfaces observed by photoemission with localized models as well.

In addition to mapping the Fermi surface, angle-resolved photoemission has also revealed unusual features near the Fermi level that may explain the microscopic origin of some of the unconventional physical properties of the high-temperature superconductors. Probably the most striking feature observed is the ubiquity of flat-band extended saddle points in the vicinity of the Fermi level in the *p*-type cuprates. At a saddle point, the band reaches a maximum along one direction and a minimum along a perpendicular direction. A simple saddle point at $(\pi, 0)$ is illustrated in Fig. 1B, corresponding to a van Hove singularity in the density of states in Fig. 1D. Saddle points in the electronic structure are not unusual, but their presence in the vicinity of the Fermi level has important physical consequences. Of the four *p*-type superconductors studied so far—Bi2212, Bi2201, $Y_2Ba_4Cu_8O_{10}$ (YBCO248), and YBCO123 (*29*, *34*, *55*)—all show a saddle point near the Fermi level. This is demonstrated in the *E* versus **k** relation in the vicinity of $(\pi, 0)$ (Fig. 5). Even though the experimental bands near $(\pi, 0)$ in Fig. 5 disperse along the same directions as the simple saddle point illustrated at $(\pi, 0)$ of Fig. 1B, the structure is quite different because of the flatness of the bands and their extent over a large region of **k** space. In fact, the observed quasi-particle dispersion is smaller than that predicted by band theory throughout the Brillouin zone. This is particularly true in the flat-band region.

The exact origin of the flat-band saddle point is still controversial. Within the context of one-electron band theory, it has been attributed to complicated band structure effects (*56*). On the other hand, the

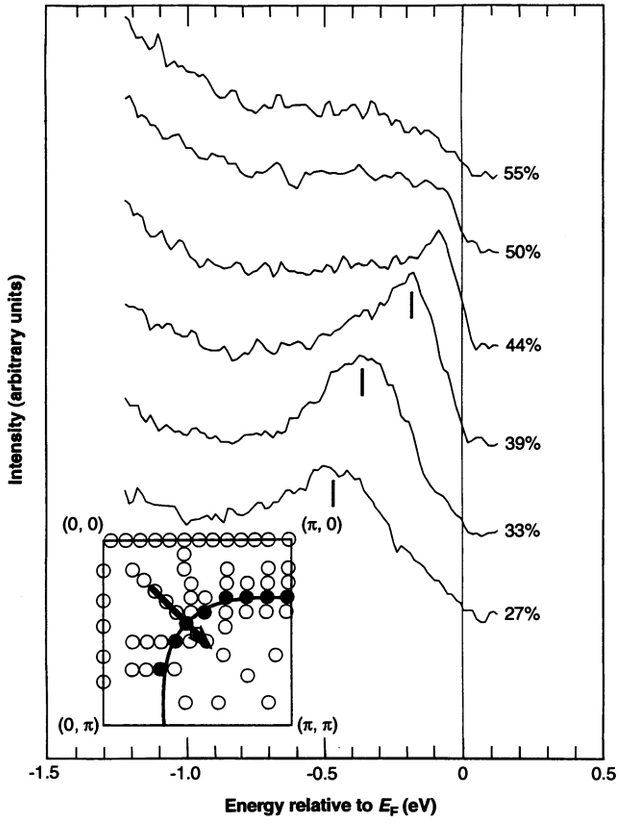

Fig. 3. The ARPES data from NCCO. Percentages indicate the distance covered from (0, 0) to (π, π). The vertical marks on the curves indicate local maxima. The inset shows the measured Fermi surface and compares it with predictions from band calculations by Massidda *et al.* (*51*) (indicated by the solid line). The circles in the inset represent the **k**-space locations that were sampled, and the dark circles show the measured Fermi surface crossing points.

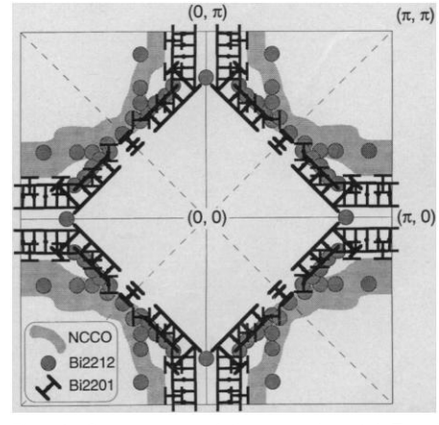

Fig. 4. Comparison of the experimental Fermi surfaces of NCCO, Bi2201, and Bi2212.

flatness of the bands could also result from many-body effects. Recent calculations of angle-resolved photoemission spectra by Bulut *et al.* (57) and Dagotto *et al.* (58), based on the Hubbard model, show flat bands at the Fermi level similar to those observed in experiments. In these calculations, the flat bands arise from the large Coulomb interaction U. Anderson suggests that the flat bands are a consequence of spin and charge excitations that are available in the highly correlated cuprates (59).

The photoemission data in Figs. 4 and 5 reveal trends that correlate well with transport properties. Figure 5 shows that the flat saddle point is very close to the Fermi energy E_F in all four p-type superconductors measured but is well below E_F for NCCO, the only n-type superconductor that has been extensively studied. This contrast agrees well with the fact that all of the p-type cuprates exhibit an unconventional linear temperature dependence of the normal-state resistivity whereas the n-type compound behaves like a normal metal, and it is consistent with models that attribute the unconventional normal-state resistivity to the presence of a saddle point at the Fermi level (60). On the other hand, the fact that Bi2201, which has a T_c of 6 to 20 K, also has a saddle point in the vicinity of the Fermi level questions the possibility of a simple connection between the presence of a van Hove singularity near E_F and a high T_c (55). It appears that NCCO has a very different electronic structure compared with other cuprate superconductors. In addition to the large energy separation between the saddle point and the Fermi level, NCCO has a simple circular Fermi surface centered at (π, π), in contrast with the nesting features in the Fermi surfaces of Bi2212 and Bi2201. The ordinary electronic structure observed in NCCO may be related to the fact that it has conventional normal and superconducting properties. Its normal-state resistivity shows a regular T^2 temperature dependence, and its superconducting gap, as measured by the London penetration depth, appears to be isotropic and agrees with the weak-coupling BCS value very well (61). It remains to be seen whether this situation is generally true for other n-type cuprates.

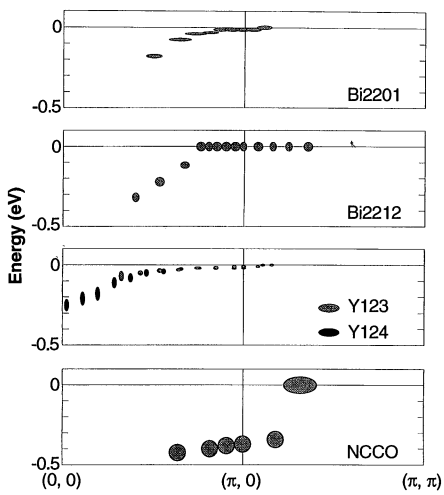

Fig. 5. E versus **k** relationship of the band near E_F for the five compounds studied (Y represents YBCO). A saddle point is seen at (π, 0).

Evolution of the Electronic Structure from Insulator to Superconductor

If one only considers the Fermi surface data from metallic samples, it is tempting to believe that we should model the electronic structure of these superconductors using a one-electron band picture (9). This scenario severs the relationship between the metals and insulators and attributes the separation to either a phase transition (26) or the creation of bandlike states near E_F with doping (24). There are, however, several reasons to question the use of the delocalized approach to describe the metallic copper oxides. First, photoemission satellite structures are present near the Cu core levels and in the valence band, indicative of the presence of a large U in metallic samples. Second, the band picture predicts a large Fermi surface, which should correspond to a high carrier density, that varies with doping like $1 - x$ (Fig. 2B). This contradicts the results of transport measurements in the low-doping regime, which reveal a carrier density proportional to x, instead of $1 - x$ (62, 63). One consequence of this discrepancy is that although NCCO appears to have a Fermi surface that encloses p-type carriers, it is found experimentally to have n-type carriers. A third reason to use the delocalized approach is that the experimentally observed band near E_F is always much narrower than that predicted everywhere in **k** space by local density approximation (LDA) calculations. It is difficult to tell just how much narrower the experimental dispersion is because the peak becomes hard to distinguish at larger binding energies and the top of the band is always unoccupied in a metal and therefore cannot be measured by photoemission. Finally, estimates for the ratio of the LDA-calculated dispersion to the experimental data vary from a factor of 2 for some measurements along (0, 0) to (π, π) (25) to a factor of 5 near the saddle point (34).

To further differentiate the localized and itinerant approaches, it is instructive to study the evolution of the electronic structure as a function of doping. The recent work by Wells *et al.* (64), which reports the disper-

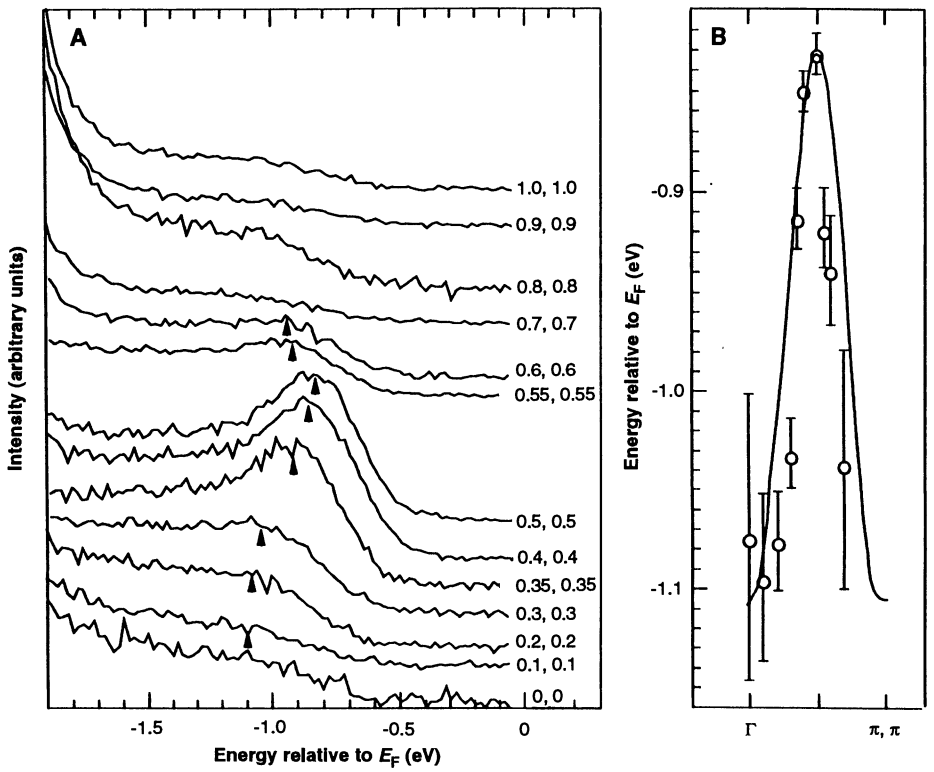

Fig. 6. (**A**) Experimental data (64) from the Mott insulator $Sr_2Cl_2CuO_2$. Each curve is labeled with the **k** position [for a square-planar Brillouin zone, in units of (π, π)] at which the data were taken. (**B**) A comparison of the data with a t-J model calculation, where J is determined from Raman experiments. The data points are marked in (A) by triangles.

sion of the single photohole in the copper oxide insulator $Sr_2CuO_2Cl_2$, pursues this idea. This compound is closely related to the high-T_c superconductors because it is a layered compound and its electronic properties are dominated by the CuO_2 planes. In fact, it has the same structure as the well-known high-T_c parent compound La_2CuO_4 and an almost identical material, $Sr_2CuO_2F_{2+\delta}$, which has recently been made superconducting (65). The study of this insulator not only gives information on the phenomenology of the doping process but also provides a test of the localized models in the insulating state, where the models are best defined. Figure 6A reproduces data by Wells *et al.* (64) along the (0, 0) to (π, π) direction. A peak disperses toward higher energy, reaches its maximum energy near ($\pi/2$, $\pi/2$), then loses intensity suddenly, and starts to move back to lower energies. The total dispersion is slightly less than 0.3 eV, which gives a rough estimate of the bandwidth. Throughout the Brillouin zone, the quasi-particle peak drops in intensity for **k** outside a line connecting (π, 0) and (0, π), the antiferromagnetic Brillouin zone boundary.

Figure 7 shows three-dimensional plots that compare the overall shape of the lowest energy bands measured in $Sr_2CuO_2Cl_2$ and that predicted by the *t-J* model as given by Dagotto *et al.* (66). The *t-J* model is a variation of the Hubbard model with infinite U that includes a t term describing electron hopping and a J term describing the magnetic interaction (67–69). In this *t-J* model, the bandwidth is predicted to be 2.2 J (70). By using an experimentally determined J from Raman scattering, we are able to compare the experimental data with no free parameters (Fig. 6B). The results in Figs. 6 and 7 show that both the calculated bandwidth and the prediction that the band reaches its maximum at ($\pi/2$, $\pi/2$) agree with the data remarkably well. The quantitative agreement between the experiment and many-body theory along the (0, 0) to (π, π) direction is significant because it shows unambiguously that the energy scale of the insulating band is controlled by J. However, the results also show that the *t-J* model cannot describe the overall shape of the band in the insulator and cannot explain the observed spectral weight effect. In addition to the *t-J* model, the Hubbard model has also been used to obtain similar dispersion relations in the intermediate coupling regime (71). In a strong coupling regime, analysis of one hole in an antiferromagnetic background shows that the band reaches a maximum at ($\pi/2$, $\pi/2$) (72).

A simple rigid band picture would predict that doping with a very small number of holes would lower the Fermi level through the band measured in $Sr_2CuO_2Cl_2$ (Fig. 7A) and produce a Fermi surface with pockets centered at ($\pi/2$, $\pi/2$). These pockets are qualitatively similar to those depicted in Fig. 2A. The key issue is understanding how the Fermi surface evolves from small pockets centered at ($\pi/2$, $\pi/2$) to a large pocket centered at (π, π) (Fig. 2B). To illustrate this, Figs. 8A and 8B show the experimental E versus **k** relations from superconducting samples of Bi2201 and NCCO. One cannot get the results in Fig. 8 by rigidly doping the bands in Fig. 7A either with electrons or holes. Although both Bi2201 and NCCO have one CuO_2 plane per unit cell, *p*- and *n*-type doping apparently each produce very different results. For *p*-type doping, an important difference in band shape between the insulator and the metal is the existence of saddle points close to the Fermi level near (π, 0) that are missing in the insulator. The near degeneracy of the flat-band saddle points near (π, 0) and the Fermi level may severely affect the shape of the Fermi surface. The development of the flat-band saddle points near the Fermi level appears to be the key to the evolution of the Fermi surface. If we consider that the bands in the region outside the antiferromagnetic Brillouin zone have very little spectral weight, as noted in Fig. 6A for **k** greater than ($\pi/2$, $\pi/2$), a many-body approach such as the *t-J* model (Fig. 7B) will produce a Fermi surface that closely resembles the observed Fermi surface of Bi2201 if oscillator strength effects are included. The results from *n*-type NCCO are much harder to reconcile using many-body theories.

The results of Wells *et al.* (64) have several very important implications. First, they reveal that the lowest energy band in the insulator and the band that crosses E_F in the hole-doped metals are very similar: The band is separated from the main valence band in the same way, it has similar dispersion, and it has similar intensity modulation as a function of energy. Thus, the dispersive

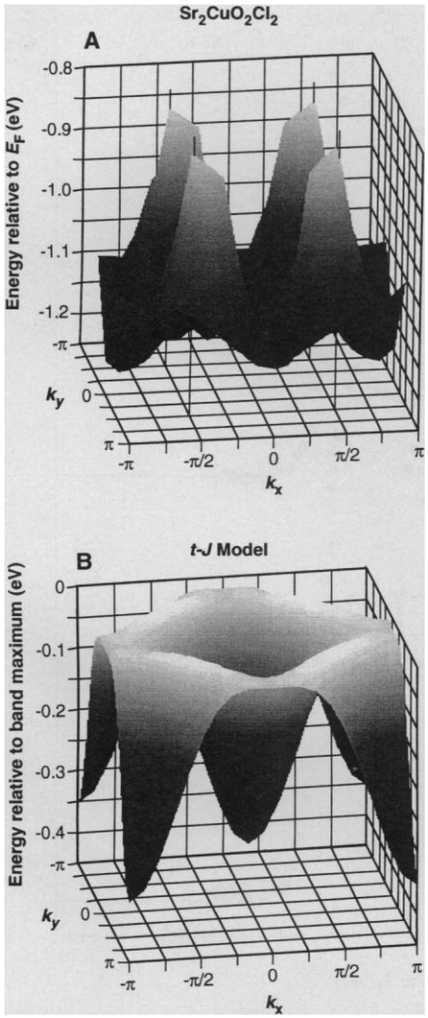

Fig. 7. The E versus **k** relation of experimental data from (**A**) $Sr_2Cl_2CuO_2$, and (**B**) the calculated results from the *t-J* model following a formula presented in (66).

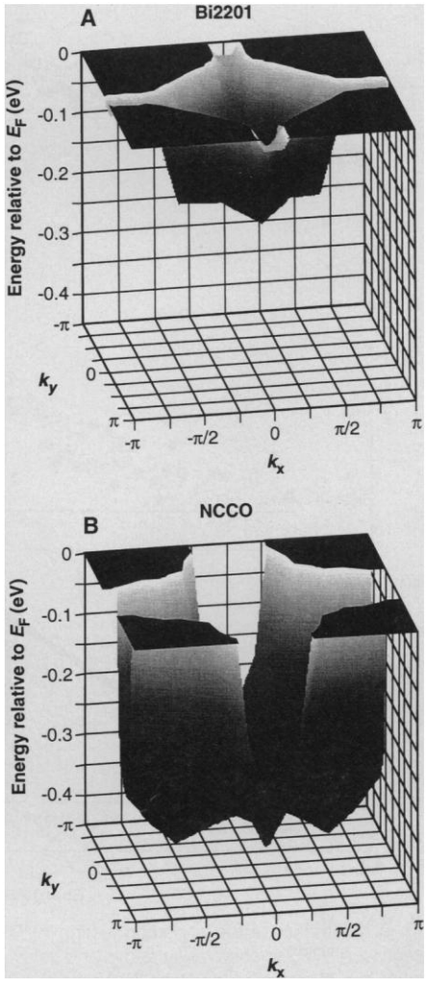

Fig. 8. The E versus **k** experimental data from (**A**) *p*-type Bi2212 and (**B**) *n*-type NCCO.

band that crosses E_F in metallic samples appears not to originate from doping and should thus be explained by the same picture in both doping regimes. Although it is not clear whether many-body theory should give small Fermi surface pockets (Fig. 2A), the decrease in oscillator strength (Fig. 6A) for **k** greater than $(\pi/2, \pi/2)$ may make part of the Fermi surface hard to observe by photoemission. We can understand this intensity change in the language of the spin-density wave (SDW) model (Fig. 2C) (*18*). The folded back "shadow band" results from the antiferromagnetic order (dashed line) and will have much less oscillator strength and spectral intensity than the original band (dotted line). Therefore, between the mixture of the two bands in the SDW state, one can see part of the band better than the others (dark solid line). This oscillator strength effect is preserved in the intermediate coupling regime (*71*) and complicates the study of the crossover from Fig. 2A to Fig. 2B. If there are small Fermi surface pockets, centered at $(\pm\pi/2, \pm\pi/2)$ in the lightly doped material (Fig. 2A), then because of the oscillator strength effect, only the side of the small Fermi surface, corresponding to the original band (dark line in Fig. 2A), will be clearly seen in a photoemission experiment. If one does not sample **k** space thoroughly, it is very difficult to distinguish Fig. 2A from Fig. 2B. This may account for the puzzling experimental data by Liu *et al.* from $YBa_2Cu_3O_x$, which shows that the band-crossing behavior along (0, 0) to (π, π) is basically the same as x varies from 6.9 to 6.4 (*26*). Therefore, the oscillator strength and shadow band Fermi surface issues are important for a comprehensive understanding of the photoemission data and provide a heuristic understanding of the subtleties in the evolution of the Fermi surface data as a function of doping. Finally, this work suggests that the electronic structure in the metallic phase may be affected by the short-range antiferromagnetic spin fluctuations (*73*), even though the effects may be very difficult to detect. Recently, Aebi *et al.* claimed to have observed such an effect (*74*), but the interpretation of the data is controversial (*75*).

We feel that the overall picture emerging from photoemission leads to the conclusion that a many-body, Hubbard-like approach is appropriate to describe the electronic structure of the cuprate superconductors. However, there are many remaining problems with the many-body theories as they stand. For example, there are no correct predictions of either the overall shape of the lowest energy band in the insulator or the evolution of the saddle point near $(\pi, 0)$ as a function of doping. Furthermore, although the *t-J* model predicts a correct dispersion and bandwidth from (0, 0) to (π, π), it cannot produce the observed oscillator strength change because the insulating gap is set to infinity in the model (*64*) and the one-band Hubbard model, as it stands now, cannot account for the observed *p*- and *n*-type asymmetry. There are also serious new attempts to improve the band calculations to better deal with the highly correlated materials. This includes the self-interaction correction, LDA + U, and other approaches (*76, 77*). These calculations have improved the LDA-calculated results in many transition-metal oxides. Unfortunately, by incorporating an ad hoc inclusion of the Coulomb repulsion U in the potentials, the calculations are no longer from first principles. At this stage, insufficient evidence exists to consistently account for the ARPES data. In summary, we continue to be puzzled by the fascinating electronic structure and physical properties, but clear progress is being made toward a coherent understanding.

Superconducting Gap Anisotropy and Its Implications

Because of the strong Coulomb interaction among conduction electrons and related antiferromagnetic spin fluctuations, unconventional pairing mechanisms have been proposed to explain superconductivity in the cuprates (*10–18*). For example, a *d*-

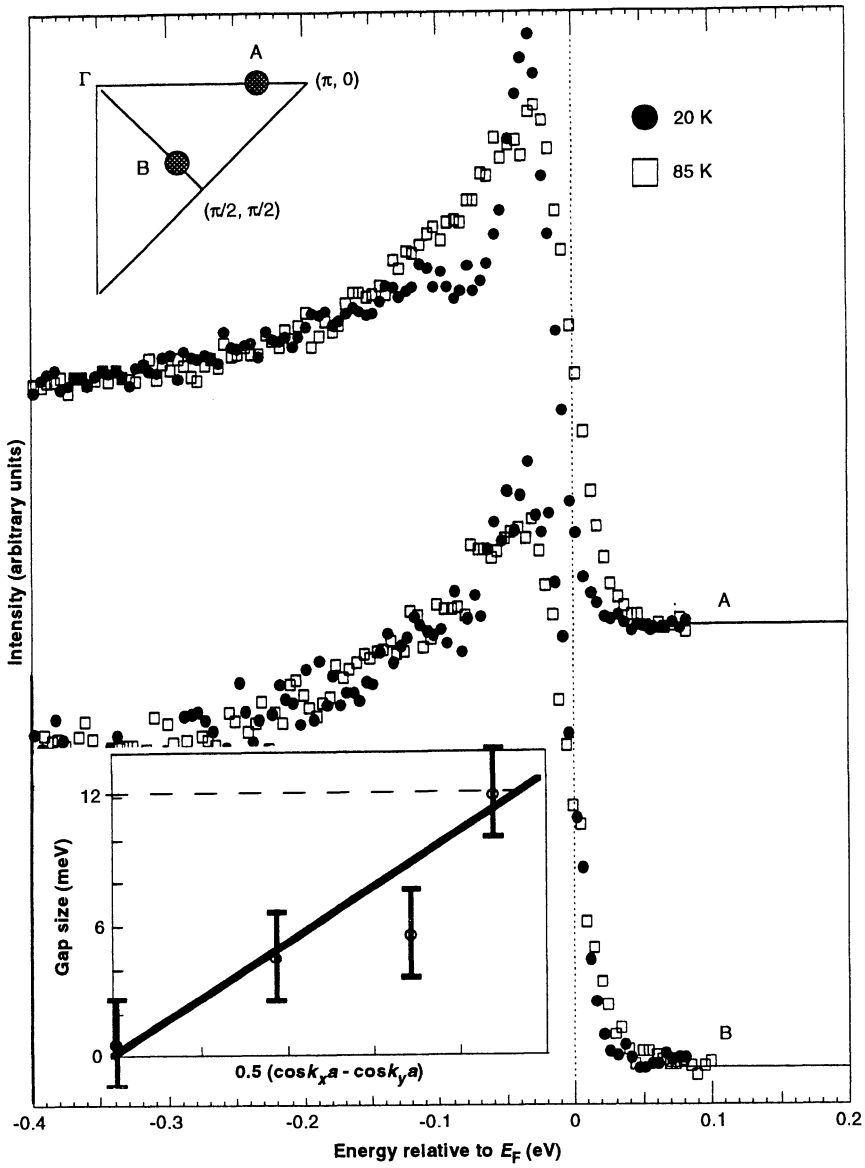

Fig. 9. Illustration of the superconducting ARPES intensity compared with the normal-state ARPES intensity. ARPES spectra taken above and below T_c (78 K) at locations where the gap is expected to be big (A) and is expected to vanish (B) by the $d_{x^2-y^2}$ pairing state. (**Inset**) Comparison of the experimental data with *d*-wave theory. The horizontal dashed line is what is expected from an isotropic *s*-wave superconductor.

wave pairing state, which has an orbital wave function with $l = 2$ angular momentum, is postulated in both the strong and the weak coupling limits (*78*). Because of the CuO_2 plane geometry, most *d*-wave theories use a $d_{x^2-y^2}$ order parameter (*10–12*, *16–18*). This order parameter requires that the gap, which is the magnitude of the order parameter, vanish along lines 45° away from the Cu–O bond direction and reach a maximum along the Cu–O bond direction. The **k** dependence of the superconducting gap, which can be measured by ARPES experiments, offers an opportunity to test the *d*-wave theories.

So far, almost all of the photoemission experiments that have detected the superconducting gap were carried out on Bi2212, presumably because of the superior surface quality. An unambiguous observation of the superconducting gap by photoemission was made by Imer *et al.* (*35*). This finding was significant because it demonstrated that photoemission could be used to study the superconducting gap. The first attempt to use angle-resolved photoemission to test the *d*-wave pairing theory was carried out by Olson *et al.* on Bi2212 (*36*). The authors found that the superconducting gap was isotropic in the **k** space sampled and thus concluded that *d*-wave theory was incorrect. More recently, with better quality samples and more systematic measurements, several groups found that the superconducting gap of Bi2212 is very anisotropic (*40–44*). Shen *et al.* (*41*) took ARPES spectra of the normal and superconducting states of a sample with T_c = 78 K (Fig. 9). The points in **k** space were chosen so that the normal-state peak is at the Fermi level, and the midpoint of the leading edge in the normal state coincides with the Fermi level at both point A along the Cu–O bond direction and point B along the line 45° away from Cu–O bond direction. Differences in the spectral change are observed at points A and B as the sample is cooled below T_c, indicating a large gap anisotropy. Quantifying the **k**-space gap anisotropy is an important but difficult task because there is not an adequate theory to describe the photoemission line shapes. For a simple measurement of the gap size, without trying to fit the peak, Shen *et al.* used the energy position of the midpoint of the leading edge of the superconducting-state spectrum. The inset in Fig. 9 displays the gap as a function of $0.5|\cos k_x a - \cos k_y a|$, where a is the lattice parameter, allowing a direct comparison with the simplest form of the $d_{x^2-y^2}$ order parameter. The data is consistent with the predictions of *d*-wave theory.

The gap anisotropy has been confirmed by subsequent experiments by several groups (*42–44*). At this point, a large gap anisotropy with a maximum along the (0, π) direction and a minimum near the (π, π) direction has been established; however, there is uncertainty whether the gap actually goes to zero along the (π, π) direction because of the limited energy resolution of photoemission. Furthermore, there is additional uncertainty from impurity scattering and surface flatness that is unresolved at this moment. On the basis of a bulk theoretical model, Norman *et al.* (*79*) attempted to interpret the scatter in the data using impurity scattering in an *s*-wave superconductor. However, we have found that the scattering is mainly caused by residual gas adsorbed on the surface (*41*, *42*). Using polarization dependence of the photoemission data, Kelley *et al.* (*80*) reported a $d_{xz + yz}$ order parameter; however, this conclusion is not compatible with other experiments (*81*).

The large gap anisotropy is consistent with the $d_{x^2-y^2}$ pairing state. However, because photoemission is not sensitive to the phase of the order parameter, it cannot distinguish between a *d*-wave and a very anisotropic *s*-wave order parameter that closely mimics the $d_{x^2-y^2}$ **k**-space dependence (*13*, *82*). A mixed symmetry state can also be consistent with the data (*14*, *15*).

Today, the question between an *s*-wave versus *d*-wave superconducting pairing state is an important issue in the field, and many experiments—including nuclear magnetic resonance, tunneling, penetration depth, Raman scattering, neutron scattering, and superconducting quantum interference measurements—have been carried out to shed light on this debate. Most of these experiments show that the superconducting gap is very anisotropic and that the anisotropy is consistent with the *d*-wave theories. To distinguish *d* wave from anisotropic *s* wave, one must resort to superconducting quantum interference experiments, which are sensitive to the phase of the superconducting order parameter. These results are becoming available from a number of different laboratories. Future photoemission experiments will benefit from increasing energy resolution and will continue to provide important results for developing theories of highly correlated systems in general and of high-T_c superconductors in particular.

REFERENCES AND NOTES

1. G. Bednorz and K. A. Muller, *Z. Phys. B* **64**, 189 (1986).
2. M. K. Wu *et al.*, *Phys. Rev. Lett.* **58**, 908 (1987).
3. N. F. Mott, *Proc. R. Soc. London Ser. A* **62**, 416 (1949).
4. J. Hubbard, *ibid.* **276**, 238 (1963).
5. P. W. Anderson, *Phys. Rev.* **115**, 2 (1959).
6. J. C. Slater, *ibid.* **82**, 538 (1951).
7. P. W. Anderson, *Science* **256**, 1526 (1992), and references therein.
8. R. B. Laughlin, *ibid.* **242**, 525 (1988), and references therein.
9. W. E. Pickett, H. Krakauer, R. E. Cohen, D. J. Singh, *ibid.* **255**, 46 (1992), and references therein.
10. D. J. Scalapino *et al.*, *Phys. Rev. B* **34**, 8190 (1986); N. E. Bickers, D. J. Scalapino, S. R. White, *Phys. Rev. Lett.* **62**, 961 (1989).
11. P. Monthoux and D. Pines, *Phys. Rev. Lett.* **67**, 3448 (1991); *ibid.* **69**, 961 (1992).
12. T. Moriya, Y. Takahashi, K. Ueda, *J. Phys. Soc. Jpn.* **59**, 2905 (1990).
13. S. Chakravarty, A. Sudbø, P. W. Anderson, S. Strong, *Science* **261**, 337 (1993).
14. D. S. Rokhsar, *Phys. Rev. Lett.* **70**, 493 (1993).
15. P. H. Dickinson and S. Doniach, *Phys. Rev. B* **47**, 11447 (1993).
16. J. R. Schrieffer, X.-G. Wen, S.-C. Zhang, *Phys. Rev. Lett.* **60**, 944 (1988).
17. P. A. Lee, *ibid.* **71**, 1887 (1993); M. U. Ubbens and P. A. Lee, *Phys. Rev. B* **49**, 6853 (1994).
18. M. Sigrist and T. M. Rice, *J. Phys. Soc. Jpn.* **61**, 4283 (1992).
19. G. Burns, *High-Temperature Superconductivity: An Introduction* (Academic Press, New York, 1992), chap. 5.
20. See articles in a recent special issue of *J. Phys. Chem. Solids* **54** (no. 10), 1073 (1993).
21. J. W. Allen and C. G. Olson, *Mater. Res. Soc. Bull.* **15** (no. 6), 34 (1990), and references therein.
22. B. W. Veal and C. Gu, *J. Electron Spectrosc. Relat. Phenom.* **66**, 321 (1994).
23. P. D. Johnson *et al.*, *Phys. Rev. B* **35**, 8811 (1987).
24. T. Takahashi *et al.*, *Nature* **334**, 691 (1988); T. Takahashi, in *Strong Correlation and Superconductivity*, H. Fukuyama, S. Maekawa, A. P. Malozemoff, Eds. (Springer-Verlag, Berlin, 1989), pp. 311–320.
25. C. G. Olson *et al.*, *Science* **245**, 731 (1989).
26. R. Liu *et al.*, *Phys. Rev. B* **45**, 5615 (1992); *ibid.* **46**, 11056 (1992).
27. J. G. Tobin *et al.*, *ibid.* **45**, 5563 (1992).
28. J. C. Campuzano *et al.*, *Phys. Rev. Lett.* **64**, 2308 (1990).
29. K. Gofron *et al.*, *J. Phys. Chem. Solids* **54**, 1193 (1993).
30. R. O. Anderson *et al.*, *Phys. Rev. Lett.* **70**, 3163 (1993).
31. R. Manzke, T. Buslaps, R. Claessen, M. Skibowski, J. Fink, *Physica C* **162–164**, 1381 (1989); G. Mante *et al.*, *Z. Phys. B* **80**, 181 (1990).
32. N. Schroeder *et al.*, *Phys. Rev. B* **47**, 5287 (1993).
33. D. M. King *et al.*, *Phys. Rev. Lett.* **70**, 3159 (1993).
34. D. S. Dessau *et al.*, *ibid.* **71**, 2781 (1993).
35. J.-M. Imer *et al.*, *ibid.* **62**, 336 (1989).
36. C. G. Olson *et al.*, *Solid State Commun.* **76**, 411 (1990).
37. B. O. Wells *et al.*, *Phys. Rev. Lett.* **65**, 3056 (1990).
38. D. S. Dessau *et al.*, *ibid.* **66**, 2160 (1991).
39. Y. Hwu *et al.*, *ibid.* **67**, 2573 (1991).
40. B. O. Wells *et al.*, *Phys. Rev. B* **46**, 11830 (1992).
41. Z.-X. Shen *et al.*, *Phys. Rev. Lett.* **70**, 1553 (1993).
42. D. S. Dessau, Z.-X. Shen, D. M. Marshall, *ibid.* **71**, 4278 (1993).
43. T. Yokoya, T. Takahashi, A. Fujiwara, Y. Koike, *Solid State Commun.* **87**, 553 (1993).
44. H. Ding *et al.*, *Phys. Rev. B* **50**, 1333 (1994).
45. We concentrate here on results from angle-resolved photoemission experiments. Angle-integrated photoemission data has been summarized before (*21*).
46. A. J. Arko *et al.*, *Phys. Rev. B* **40**, 2268 (1989).
47. J. C. Fuggle *et al.*, *ibid.* **37**, 123 (1988).
48. A. Fujimori, E. Takayama-Muromachi, Y. Uchida, B. Okai, *ibid.* **35**, 8814 (1987).
49. Z.-X. Shen *et al.*, *ibid.* **36**, 8414 (1987).
50. C. A. R. Sa de Melo and S. Doniach, *ibid.* **41**, 6633 (1990).
51. S. Massidda, N. Hamada, J. Yu, A. J. Freeman, *Physica C* **157**, 571 (1989).
52. The Fermi surface of YBCO123 has also been studied by Liu *et al.* (*26*); the physical picture we will discuss is basically the same.
53. J. Ruvalds, C. T. Rieck, J. Zhang, A. Virosztek, *Science* **256**, 1664 (1992); A. Virosztek and J. Ruvalds, *Phys. Rev. B* **42**, 4064 (1990).
54. R. J. Birgeneau *et al.*, *Z. Phys. B* **87**, 1 (1992).
55. D. M. King *et al.*, *Phys. Rev. Lett.* **73**, 3298 (1994).
56. S. Gopalan, O. Gunnarsson, O. K. Andersen, *Phys. Rev. B* **46**, 11798 (1992).

57. N. Bulut, D. J. Scalapino, S. White, *Phys. Rev. Lett.* **72**, 705 (1994).
58. E. Dagotto, A. Nazarenko, M. Boninsegni, *ibid.* **73**, 728 (1994).
59. P. W. Anderson, *J. Phys. Chem. Solids* **54**, 1073 (1993), and references therein.
60. This connection has been made by many authors, as shown in the review D. M. Newns *et al.*, *Comments Condens. Matter Phys.* **15**, 273 (1992), and references therein.
61. D. H. Wu *et al.*, *Phys. Rev. Lett.* **70**, 85 (1993).
62. See overview articles in *Phys. Today* **44** (no. 6), 1 (1991).
63. N. P. Ong *et al.*, *Phys. Rev. B* **35**, 8807 (1987); N. P. Ong, in *Physical Properties of the High-Temperature Superconductors*, vol. 2, D. M. Ginsberg, Ed. (World Scientific, Singapore, 1990).
64. B. O. Wells *et al.*, in press.
65. M. Al-Mamouri *et al.*, *Nature* **369**, 382 (1994).
66. E. Dagotto *et al.*, *Phys. Rev. B* **41**, 9049 (1990); E. Dagotto, *Rev. Mod. Phys.* **66**, 763 (1994).
67. F. C. Zhang and T. M. Rice, *Phys. Rev. B* **37**, 3759 (1988).
68. H. Eskes, M. B. Meinders, G. A. Sawatzky, *Phys. Rev. Lett.* **67**, 1035 (1991).
69. R. B. Laughlin, *Proceedings of VI Physics Summer School, Canberra, Australia*, M. P. Das and J. Mahanty, Eds. (World Scientific, Singapore, 1994), p. 294.
70. Z. Liu and E. Manousakis, *Phys. Rev. B* **45**, 2425 (1992).
71. N. Bulut, D. J. Scalapino, S. R. White, *Phys. Rev. Lett.* **73**, 748 (1994).
72. S. A. Trugman, *Phys. Rev. B* **37**, 1597 (1988).
73. A. P. Kampf and J. R. Schrieffer, *J. Phys. Chem. Solids* **52**, 1321 (1991).
74. P. Aebi *et al.* , *Phys. Rev. Lett.* **72**, 2757 (1994).
75. S. Chakravarty, preprint.
76. V. I. Anisimov *et al.*, *Phys. Rev. Lett.* **68**, 345 (1992).
77. A. Svane and O. Gunnarsson, *ibid.* **65**, 1148 (1990); A. Svane, *ibid.* **68**, 1900 (1992).
78. D. J. Scalapino, in press.
79. M. Norman *et al.*, unpublished data.
80. R. J. Kelley, J. Ma, G. Margaritondo, M. Onellion, *Phys. Rev. Lett.* **71**, 4051 (1993).
81. D. S. Dessau *et al.*, preprint.
82. G. D. Mahan, *Phys. Rev. Lett.* **71**, 4277 (1993).
83. We acknowledge the stimulating discussions with R. B. Laughlin, S. Doniach, D. J. Scalapino, J. Ruvalds, P. W. Anderson, P. Littlewood, and S. C. Zhang. The Stanford Synchrotron Radiation Laboratory is operated by the Department of Energy (DOE) Office of Basic Energy Science, Division of Chemical Sciences. The Office's Division of Materials Science has provided support for this research. The Stanford work was also supported by National Science Foundation (NSF) grants DMR9121288 and DMR9357057 and the NSF grant through the Center of Materials Research. Z.X.S. would like to acknowledge support from the Alfred P. Sloan foundation and D.S.D. would like to acknowledge support from a DOE Distinguished Postdoctoral Research Fellowship.